

---

# (4, 4′)-Bipyridine in vacuo and in solvents: A quantum chemical study of a prototypical floppy molecule from a molecular transport perspective †¶

Ioan Bâldea,<sup>\*a‡</sup> Horst Köppel,<sup>a</sup> and Wolfgang Wenzel<sup>b</sup>

DOI: 10.1039/C2CP43627B

We report results of quantum chemical calculations for the neutral and anionic species of (4, 4′)-bipyridine (44BPY), a prototypical molecule with a floppy degree of freedom, placed in vacuo and in solvents. In addition to equilibrium geometries and vibrational frequencies and spectra, we present adiabatic energy curves for the vibrational modes with significant intramolecular reorganization upon charge transfer. Special attention is paid to the floppy strongly anharmonic degree of freedom of 44BPY, which is related to the most salient structural feature, namely the twist angle  $\theta$  between the two pyridine rings. The relevance of the present results for molecular transport will be emphasized. We show that the solvent acts as a selective gate electrode and propose a scissor operator to account for solvent effects on molecular transport. Our result on the conductance  $G$  vs.  $\cos^2 \theta$  is consistent with a significant transmission in perpendicular conformation indicated by previous microscopic analysis.

## 1 Introduction

The present work represents a quantum chemical study intended to pave the way toward microscopic nanotransport studies in single-molecule devices in vacuo and in solvents based on (4, 4′)-bipyridine (44BPY), a prototypical floppy molecule, wherein a floppy vibrational mode turns out to yield an important intramolecular reorganization upon charge transfer. This is an effect, which existing transport studies did not consider.

In view of its special structure, 44BPY is a representative model molecule that attracted considerable experimental and theoretical interest. Compounds based on 44BPY, commonly known as viologens, captured chemists' attention for many decades, especially due to their electrochemically reversible behavior.<sup>1,2</sup> They have been investigated from various perspectives, like herbicidal activity,<sup>3</sup> electrochemical display devices, storage energy, catalytic oxidation,<sup>3-6</sup> photoactive molecular, and supramolecular machines.<sup>7</sup> The preparation of complexes embedding neutral, radical anionic and dianionic forms of (4, 4′)-bipyridyl ligands is of interest for designing switchable materials wherein the redox chemistry can be finely matched to facilitate electron transfer.

More recently, the 44BPY molecule has been used in

molecular electronics.<sup>8-10</sup> Due to its special structure, with two active nitrogen atoms in para positions (cf. Fig. 1), 44BPY is particularly suitable for simultaneous binding to metallic electrodes. This fact has been exploited in the first work that succeeded in the repeated formation of numerous molecular junctions.<sup>9</sup> 44BPY molecules have been incorporated in redox active tunneling junctions to demonstrate the electrolyte gating.<sup>10</sup>

It is from the perspective of molecular electron transport that the present quantum chemical study has been conducted. Unlike in most molecular electronic devices fabricated so far, in the single-molecule junctions based on 44BPY there exists clear experimental evidence that the electric current is due to negatively charged carriers (n-type conduction): the measured Seebeck coefficient is negative.<sup>11</sup> This indicates that the electron tunneling through molecular junctions wherein a 44BPY molecule is contacted to gold electrodes is predominantly due to the lowest unoccupied molecular orbital (LUMO). A positive Seebeck coefficient, with the associated p-type conduction, would have revealed the predominance of the highest occupied molecular orbital (HOMO). As a further support, one can invoke the results on electrochemical gate-controlled electron transport through redox-active viologen molecular junctions,<sup>10</sup> which also indicate a LUMO-mediated conduction. This kind of experiments also enables one to distinguish between electron (LUMO-mediated) n-type conduction and hole (HOMO-mediated) p-type conduction: the gate potential (overpotential in electrochemists' nomenclature) shifts the energies of the occupied and unoccupied molecular orbital in opposite directions relative to the electrodes' Fermi level, enhancing or diminishing the electric current.

---

† Electronic Supplementary Information (ESI) available: Additional details and tables. See DOI: 10.1039/C2CP43627B

¶ Published: Phys. Chem. Chem. Phys. 2013, 15, 1918–1928

<sup>a</sup> Theoretische Chemie, Universität Heidelberg, Im Neuenheimer Feld 229, D-69120 Heidelberg, Germany.

<sup>‡</sup> E-mail: ioan@pci.uni-heidelberg.de. Also at National Institute for Lasers, Plasmas, and Radiation Physics, ISS, Bucharest, Romania

<sup>b</sup> Institut für Nanotechnologie, Karlsruher Institut für Technologie (KIT), D-76131 Karlsruhe, Germany

By implication, this means that, when an electron subjected to a source-drain voltage travels across a 44BPY-based molecular junction, a transient radical anion ( $44\text{BPY}^{\bullet-}$ ) is formed. Therefore, the determination of the properties of the neutral  $44\text{BPY}^0$  molecule as well as of the bipyridyl radical  $44\text{BPY}^{\bullet-}$  is a prerequisite for understanding the electron transport in these molecular junctions. This is the aim of the present paper.

The quantum chemical calculations reported below have been performed by using the Gaussian 09 suite of programs<sup>12</sup> at DFT/B3LYP level. Our study substantially goes beyond earlier works wherein both the parent molecule  $44\text{BPY}^0$  and the radical anion  $44\text{BPY}^{\bullet-}$  have been investigated theoretically, the latter especially in relation with photoreduction.<sup>13–20</sup> The aforementioned theoretical works used smaller basis sets and only considered a few ground state properties of  $44\text{BPY}^0$  and  $44\text{BPY}^{\bullet-}$  in vacuo. In addition to the case of vacuum, we also present results for 44BPY in solvents of experimental interest. The solvent has been described within the polarized continuum model using the integral equation formalism (keyword SCRF=IEFPCM in Gaussian 09). For the anionic (and cationic, cf. Sec. 5) species, we carried out unrestricted calculations (Gaussian keyword UB3LYP). Because calculations for open shell systems can sometimes be problematic (wrong geometries, spurious symmetry breaking, or spin contamination, see, e. g., Ref. 21), to avoid artefacts we always checked our results carefully, and convinced ourselves that, for instance, optimizations properly converged (all frequencies are real), symmetries (point group  $D_2$  for  $44\text{BPY}^0$  and  $44\text{BPY}^{\bullet+}$ , and  $D_{2h}$  for  $44\text{BPY}^{\bullet-}$ ) and spin are correct. For concreteness, we mention that, with the default settings of Gaussian 09, typical spin values found are  $\langle S^2 \rangle = 0.7592$  before annihilation of the first contaminant and  $\langle S^2 \rangle = 0.7501$  after annihilation. To be complete, let us still note that no problem arose even in the “small” calculation for the anion done at the very modest ROHF/6-31g(+\*) level of theory (cf. end of Sec. 3); that calculation has been solely done to allow comparison with and check results of earlier work.

The remaining part of this paper is organized as follows. In Section 2, results for the equilibrium geometries of the neutral and anionic species obtained by using basis sets larger than those employed in previous studies will be reported. Further, vibrational effects in the radical anion placed in vacuo and in experimental conditions (acetonitrile as solvent<sup>17</sup>) will be discussed in Section 3. Section 4 is devoted to an analysis of the relevant adiabatic energy curves for  $44\text{BPY}^0$  and  $44\text{BPY}^{\bullet-}$ ; this analysis is augmented with the discussion in the Electronic Supplementary Information. Results for the 44BPY molecule immersed in solvents will be presented in Section 5. Because the present quantum chemical investigation is intended to pave the way toward transport studies in 44BPY-based molecular devices, we present in Section 6 preliminary results revealing the impact of the molecular conformation on

the electrical conductance. Discussions and conclusions will be presented in Section 7.

## 2 Equilibrium geometries of $44\text{BPY}^0$ and $44\text{BPY}^{\bullet-}$

In this study, quantum chemical calculations for geometry optimizations without imposing any constraints have been performed both for the neutral and for the anionic species. In such calculations, an important issue is to employ a sufficiently large basis set.

We have extensively investigated the impact of the basis set size. Table S1 (tables with label S are from the Electronic Supplementary Information) collects our results on the equilibrium geometry of the neutral 44BPY molecule obtained via DFT/B3LYP and various basis sets. The atom numbering is given in Fig. 1. The optimum geometry of the neutral

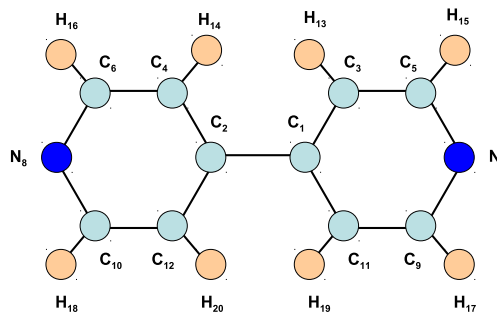


**Fig. 1** The (4,4') molecule ( $44\text{BPY}$ ) and the atom numbering used in the present work.

species has been previously investigated in a series of studies.<sup>13,14,17,18,20,22</sup> These studies used lower theoretical levels (semi-empirical, HF) and/or smaller basis sets (sto-3g, 3-21g(+\*), 6-31g(+\*)<sup>23</sup>). As compared to those results, our results represent an improved agreement with experiment.<sup>24,25</sup> For the cc-pVTZ basis set, the largest set used earlier for  $44\text{BPY}^0$ ,<sup>19</sup> our study basically confirms the results reported in Ref. 19. We note that there exist small differences between the present geometrical parameter values computed with Gaussian 09 and those (also included in Table S1) computed with GAMESS in Ref. 19 at the same DFT/B3LYP/cc-pVTZ level

of theory. However, they are small; bond lengths differ by at most 0.001 Å. By and large, Table S1 confirms the previous claim<sup>18</sup> that the geometrical parameters of 44BPY<sup>0</sup> are little sensitive to the basis set size. An important fact to be emphasized in connection to Table S1 is that, while substantially increasing the computational cost, the usage of larger basis sets does not necessarily improve the agreement between theoretical and experimental bond metric data. For instance, although the inter-ring C–C bond length is somewhat reduced by increasing the basis set, it remains slightly larger than the experimental one.<sup>25</sup> The theoretical value becomes closer to a normal C(sp<sup>2</sup>)–C(sp<sup>2</sup>) single bond (1.479 Å).<sup>26</sup>

Most sensitive to the basis set size is the twisting angle  $\theta = \widehat{C_3C_1C_2C_4}$  between the two pyridyl rings, which has been long recognized to be the salient structural feature of this molecule,<sup>13,14,17,18</sup> whose variations are related to very small energy variations.

Our bond metric data for the radical anion 44BPY<sup>•−</sup> are shown in Table S2. One should note that the previous theoretical studies on the anion have been done either semi-empirically<sup>15</sup> or by using much smaller basis sets (HF/3-21g(+\*)<sup>17</sup> and DFT/6-31g(+\*)<sup>18,23</sup>). In the absence of direct experimental results for the anion structure, we can only present the comparison with existing theoretical results obtained for the largest basis, namely 6-31 g(+\*) of Ref. 18. Somewhat surprisingly, the geometrical parameters are little sensitive to the basis set size even in the case of the radical anion 44BPY<sup>•−</sup>. Noteworthy, the computed geometrical parameters are rather insensitive to the presence of the diffuse basis functions. This behavior contrasts with that exhibited by other properties of the anion, which will be examined later in Sections 4 and 6.

Because the structural differences between the neutral molecule 44BPY<sup>0</sup> and its reduced form 44BPY<sup>•−</sup> have been amply discussed in the literature (see, e. g., Refs. 17,18 and 27), we only briefly mention the main aspects. The twisting angle  $\theta$  between the two pyridyl rings results from the interplay between the  $\pi$ -electronic interaction of the pyridyl fragments and the steric repulsion of the ortho hydrogen atoms (H<sub>13</sub> and H<sub>14</sub>, and H<sub>19</sub> and H<sub>20</sub> in Fig. 1). The former favors a planar conformation ( $\theta = 0$ ) wherein the  $\pi$ -electrons are delocalized between the pyridyl rings, while the latter prefers a nonplanar conformation ( $\theta \neq 0$ ) wherein the steric hindrance is reduced. The neutral molecule can be characterized as consisting of two aromatic pyridyl rings linked by a (nearly) single C–C bond in a twisted conformation (point group D<sub>2</sub>). The balance between the two aforementioned effects in the neutral molecule yields an equilibrium value  $\theta_{eq} = 37.2^\circ$ , as measured in electron diffraction experiments,<sup>24</sup> which can be well reproduced by quantum chemical calculations (cf. Table S1).

As suggested for the first time on the basis of a semi-empirical MO approach,<sup>15</sup> and later within HF/3-21g(+\*)<sup>17</sup>

and DFT/6-31g(+\*)<sup>18</sup> calculations, two important structural changes occur on going from the parent molecule 44BPY<sup>0</sup> to the radical anion 44BPY<sup>•−</sup>. First, the  $\pi$ -electronic interaction is enhanced by the extra electron delocalized over the reduced molecule, which becomes planar ( $\theta_{eq} = 0$ , point group D<sub>2h</sub>). Second, the anion is characterized by a (planar) quinoidal structure. Basically, the quinoidal distortion is localized in the inter-ring region. On going from the neutral to the reduced species, mostly affected are the inter-ring C<sub>1</sub>–C<sub>2</sub> bond length, which shortens by  $\sim 0.052$  Å, becoming thereby substantially stronger and acquiring partial double bond character (bond order 1.247, see below), and the neighboring C<sub>1</sub>–C<sub>3</sub> bond length, which increases by  $\sim 0.034$  Å. Less affected are the C<sub>5</sub>–N<sub>7</sub> bond, which lengthens by  $\sim 0.018$  Å, and the C<sub>3</sub>–C<sub>5</sub> ring bond, which shortens by  $\sim 0.012$  Å. The calculated bond orders are only slightly dependent on the method. With ROHF/6-31g(+\*) we found 1.288 and 1.532 for C<sub>1</sub>–C<sub>2</sub>- and C<sub>3</sub>–C<sub>5</sub>-(Wiberg) bond order indices, confirming thereby the previously reported values 1.29 and 1.53, respectively;<sup>28</sup> B3LYP/aug-cc-pVTZ yields the values 1.247 and 1.560, respectively.<sup>29</sup>

### 3 Vibrational modes of the radical anion 44BPY<sup>•−</sup>

For the neutral 44BPY molecule, theoretical results obtained by using DFT/B3LYP and good basis sets (e. g., cc-pVTZ<sup>19</sup>) have already been compared with the experimental data available for the Raman<sup>17</sup> and infra-red (IR) active<sup>17,20</sup> vibrational modes. By using basis sets larger (cf. Table S1) than that employed in Ref. 19, we did not find a significant improvement against experiments: the empirical factors, which are commonly introduced<sup>30,31</sup> to scale the calculated vibrational frequencies, remain close to the value  $\sim 0.98$  found in Ref. 19.

Therefore, we confine ourselves to discuss vibrational effects for the radical anion, wherein earlier results<sup>17,18</sup> have been obtained at modest theoretical levels (HF/3-21g(+\*)<sup>17</sup> and DFT/B3LYP/6-31G(+\*)<sup>18</sup>). The results for the frequencies of the Raman active modes, which can be compared with available experimental data,<sup>17</sup> are collected in Table S3. Although Raman measurements have also been carried out for the partially or totally deuterated radical anion<sup>17</sup>, we confine ourselves to the undeuterated case, of more direct relevance for electron transport. The Raman measurements<sup>17</sup> comprise the spectral range  $300 \text{ cm}^{-1} < \omega < 2000 \text{ cm}^{-1}$ . It does not include the spectral range  $\omega > 3000 \text{ cm}^{-1}$  wherein C–H stretching modes are active (see Figs. 2 and 3). Out of the eight Raman active modes (A<sub>g</sub> symmetry) shown in Table S3, only seven have been detected experimentally.<sup>17</sup> The lowest ring deformation mode (6a, cf. Table S3) has not been observed. This can be understood: the spectra calculated by us (Fig. 2)

show indeed a very weak spectral intensity for this mode.

As compared with the approach HF/3-21g(+\*) of Ref. 17, where the empirical scaling factor amounts 0.892, the approach of Ref. 18 already represented a substantial improvement: the empirical scaling factor needed there was substantially larger ( $f_{sc} = 0.968$ ). The agreement is further improved by using larger basis sets, as expressed by the values  $f_{sc} \simeq 0.98$  of Table S3. So, the agreement is basically as good as that for the neutral molecule. To conclude, the DFT approach is able to accurately reproduce experimental vibrational frequencies: the deviations amount to  $\sim 2\%$ ; for the modes shown in Table S3 this represents an absolute deviation of  $\sim 10 - 30 \text{ cm}^{-1}$ . One should still note that, similar to the case of the geometrical parameters, further improvement cannot be achieved by employing larger basis sets (for aug-cc-pVQZ, we found  $f_{sc} = 0.980$ ), a fact which reflects the intrinsic limitation of the current theory.

In contrast to the fact, already noted, of relatively insensitive vibrational frequencies, the Raman intensities are much more sensitive to the basis set. This is exemplified by the Raman spectrum presented in Fig. 2.<sup>32</sup>

Because the Raman measurements refer to the anion in solvent (acetonitrile),<sup>17</sup> we have also performed calculations for this situation. As visible in Table S3 and Fig. 2, while weakly affecting the vibrational frequencies, the solvent has a significant impact on the spectral Raman intensities.

Although we are not aware of experimental studies on vibrational spectra of the infra-red (IR) active modes in the radical anion 44BPY<sup>•-</sup>, for completeness we have also calculated the IR spectrum. These results are presented in Fig. 3. As compared to the Raman spectra, the IR spectra depicted in Fig. 3 turn out to be much less affected both by the basis set size and by the presence of the solvent.

#### 4 Adiabatic ground state energy curves of 44BPY<sup>0</sup> and 44BPY<sup>•-</sup>

The coherent electron transport through single-molecule junctions based on 44BPY was investigated theoretically in several works.<sup>11,33-35</sup> In spite of significant differences between them, there is a common finding in those studies, namely that the coherent electron transport is determined by the LUMO: close to the metallic Fermi energy, the calculated transmission exhibits a single pronounced Lorentzian peak and the Seebeck coefficient is negative. The LUMO energy can be obtained from electronic structure  $\Delta$ -DFT calculations: it represents the difference between the anion and neutral ground state energies  $E_{LUMO} = E_A - E_N$  at the neutral equilibrium geometry  $\mathbf{Q}_N$ .<sup>36</sup>

Refs. 11,33-35 assumed a molecular geometry frozen at  $\mathbf{Q} = \mathbf{Q}_N (\equiv \mathbf{0})$ . Our recent study<sup>27</sup> drew attention to the fact that intramolecular reorganization is important and should

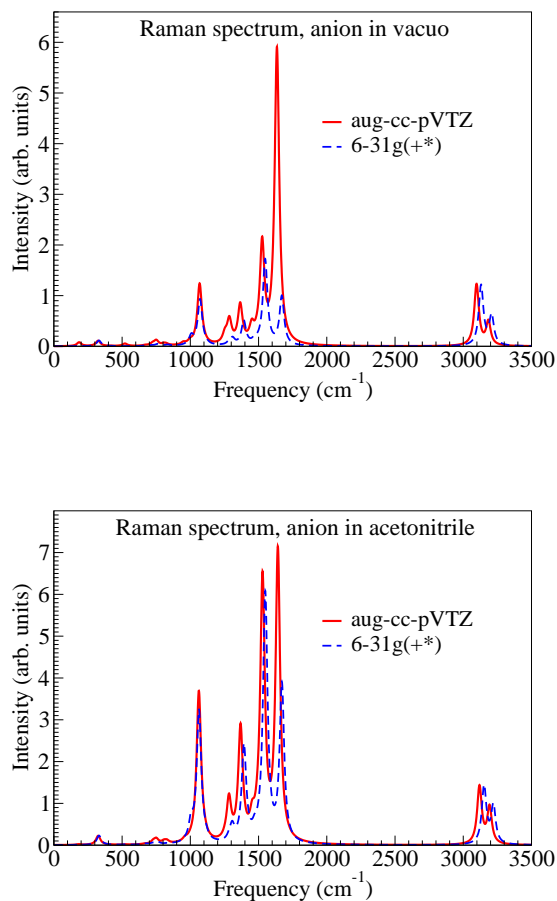


**Fig. 2** Theoretical Raman spectra calculated with the basis sets 6-31g(+\*)<sup>23</sup> and aug-cc-pVTZ for the radical anion 44BPY<sup>-1</sup> placed in vacuo and acetonitrile. They illustrate that both the basis set size and the solvent significantly affect the Raman spectral intensities. The computed spectral lines have been convoluted with Lorentzian functions of half-width  $20 \text{ cm}^{-1}$ . See the main text for details.

be considered, especially because the 44BPY molecule possesses a floppy degree of freedom. In particular, this implies that the LUMO energy is not fixed at the value  $E_{LUMO} = E_A(\mathbf{Q}_N) - E_N(\mathbf{Q}_N)$ . Instead, one should consider a distribution of values  $E_{LUMO}(\mathbf{Q}) = E_A(\mathbf{Q}) - E_N(\mathbf{Q})$ , and perform a  $\mathbf{Q}$ -ensemble averaging of the current computed at various molecular geometries  $\mathbf{Q}$ . The weight function needed for this ensemble averaging requires the knowledge of the adiabatic

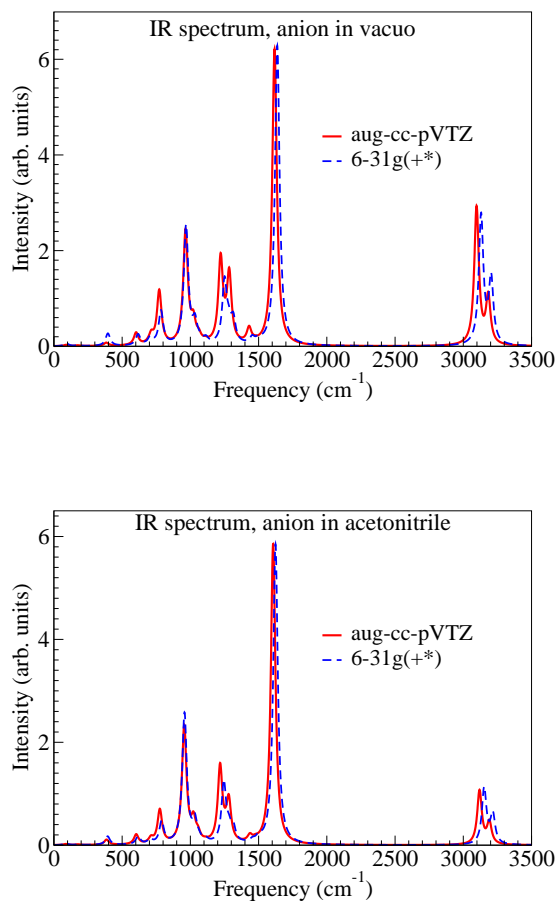


**Fig. 3** Theoretical IR spectra calculated with the basis sets 6-31g(+\*)<sup>23</sup> and aug-cc-pVTZ for the radical anion 44BPY<sup>-1</sup> placed in vacuo and acetonitrile. They illustrate that neither the basis set size nor the solvent drastically affect the spectral intensities. The computed spectral lines have been convoluted with Lorentzian functions of half-width 20 cm<sup>-1</sup>. See the main text for details.

Gibbs free energy surface  $\mathcal{G}(\mathbf{Q})$ . The calculation of  $\mathcal{G}(\mathbf{Q})$  is nontrivial (cf., e. g., Refs. 27,37 and citations therein). Necessary (but not sufficient) quantities that should be determined from electronic structure calculations are the adiabatic potential energy surfaces  $E_{N,A}(\mathbf{Q})$  of the neutral and anion electronic ground states at arbitrary geometries  $\mathbf{Q}$ , as has been done in the present work.

Applied to the case considered here, intramolecular reorganization manifests itself in the different locations  $\mathbf{Q}_A \neq \mathbf{Q}_N$

of the minima of the adiabatic energy surfaces  $E_A(\mathbf{Q})$  and  $E_N(\mathbf{Q})$ , respectively. The reorganization energies  $\lambda_{N,A}$  of the neutral and anionic species represent important quantities for electron transport both in the nonadiabatic (Mulliken-Hush-Marcus-type)<sup>38–40</sup> and adiabatic<sup>27,37,41–43</sup> limits. They are defined as

$$\begin{aligned}\lambda_N &= E_N(\mathbf{Q}_A) - E_N(\mathbf{Q}_N), \\ \lambda_A &= E_A(\mathbf{Q}_N) - E_A(\mathbf{Q}_A).\end{aligned}\quad (1)$$

Our calculations confirm the intuitive expectation that significant contributions to the reorganization energy arise from the totally symmetric in-plane normal modes. The Raman active vibrational modes included in Table S3 belong to these modes. Out of them, the largest contribution to the reorganization energy comes from the mode 8a. Adiabatic energy curves  $E_{N,A}(Q_{8a})$  along the normal coordinate  $Q_{8a}$  (all the other  $\mathbf{Q}$ 's being set to zero) are presented in Fig. 4 and indicate a virtually perfect harmonic behavior.

Considered alone, each of the Raman active modes other than 8a listed in Table S3 has a small contribution to reorganization and also exhibits a harmonic behavior. Their contribution can be accounted for by a renormalization factor of mode 8a  $f_h$  ( $\omega_{8a} \rightarrow \tilde{\omega}_h = f_h \omega_{8a}$ ), as discussed in the Electronic Supplementary Information.<sup>44</sup> In accord with a general property of the harmonic modes,<sup>27</sup> the corresponding partial reorganization energies for the neutral and anionic species should be equal. For the mode 8a alone, we found  $\lambda_N^{8a} = \lambda_A^{8a} = 0.0845$  eV.

However, the values of the total reorganization energies  $\lambda_{N,A}$  computed from Eq. 1 were found different,  $\lambda_N \simeq 0.23$  eV and  $\lambda_A \simeq 0.35$  eV, and this inequality traces back to the lowest frequency mode, which is strongly anharmonic.<sup>27</sup> This mode is directly related to the inter-ring torsional motion and represents the floppy (label  $f$ ) degree of freedom of the 44BPY molecule.<sup>27</sup> Its frequency  $\omega_f \simeq 62$  cm<sup>-1</sup><sup>27</sup> lies well below the spectral vibrational range investigated experimentally ( $400$  cm<sup>-1</sup>  $\lesssim \omega \lesssim 1800$  cm<sup>-1</sup>) for 44BPY<sup>0,20</sup> and  $300$  cm<sup>-1</sup>  $\lesssim \omega \lesssim 2000$  cm<sup>-1</sup>) for 44BPY<sup>•-1</sup>.<sup>17</sup> However, in spite of this very low frequency, its contribution to the reorganization energy is important because of the large amplitude vibrations associated with it. The anionic and neutral adiabatic energy curves along the coordinate  $Q_f$  of the neutral molecule, which are depicted in Fig. 5, exhibit strong anharmonicities. The fact that strong anharmonic effects characterize molecules possessing floppy degrees of freedom is well known (see, e. g., Ref. 45). However, except for the preliminary work of Ref. 27, we are not aware of (transport-related) studies drawing attention to the fact that such modes can be strongly coupled to molecular orbitals with essential contribution to the charge transfer.

In Fig. 6, we present adiabatic curves  $E_{N,A}(Q_f)$  for the neutral and anionic species calculated with various basis sets. The

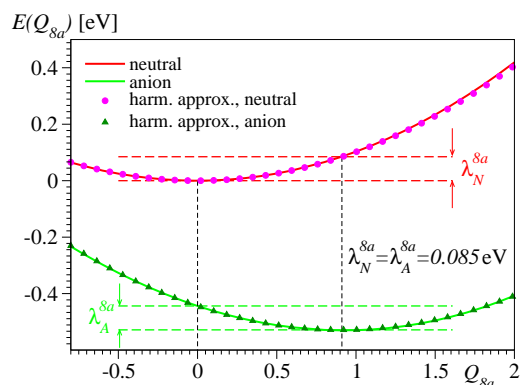


**Fig. 4** Adiabatic energy curves along the coordinate  $Q_{8a}$  of mode 8a of the neutral molecule ( $\omega_{8a}^N = 1640 \text{ cm}^{-1}$ ) computed with the basis set aug-cc-pVDZ for neutral 44BPY and radical anion bipyridyl 44BPY $^{\bullet-}$ . Notice the almost perfect harmonic behavior and the fact that the neutral and anion minima are located on the same side with respect to the intersection point of the curves, situated at left beyond the figure's frame (inverted regime).

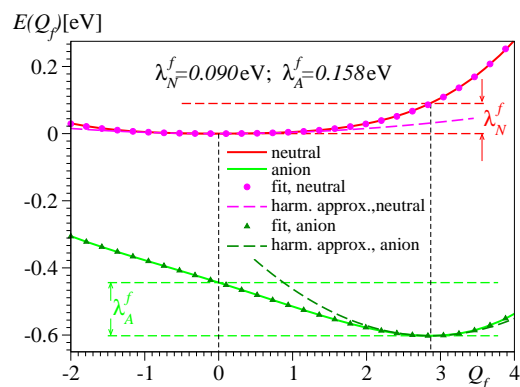


**Fig. 5** Adiabatic energy curves along the coordinate  $Q_f$  of the neutral molecule of the lowest frequency mode ( $\omega_f = 62 \text{ cm}^{-1}$ ) computed with the basis set aug-cc-pVDZ for neutral 44BPY and radical anion bipyridyl 44BPY $^{\bullet-}$ . Notice the strong departures from curves corresponding to the harmonic approximation. See the main text for details.

inspection of these curves reveals an important difference between the neutral and anionic species. The adiabatic curves of the neutral molecule are weakly affected by the basis set employed in the calculations; essentially, this dependence is similar to the geometrical parameters and the vibrational fre-

quencies presented in the Electronic Supplementary Information. On the contrary, the adiabatic curves of the radical anion exhibit a pronounced dependence on the basis set. A closer look at the  $E_A(Q_f)$ -curves reveals that it is not the size of the basis set that matters; of primary importance is to include diffuse basis functions. For example, the results obtained by using the cc-pVTZ basis set are much poorer than by using the rather modest 6-31+g(d) basis set. Noteworthy is also the fact that an anion unstable against electron autodetachment (i. e.,  $E_A > E_N$ ) can be the (incorrect) result of using an inadequate basis set; this aspect has already been pointed out.<sup>17,18</sup>

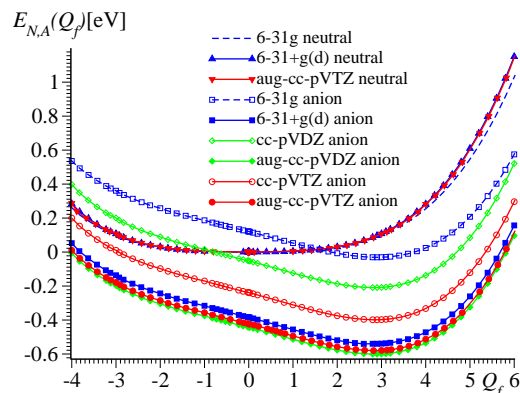


**Fig. 6** The adiabatic energy curves  $E_{N,A}(Q_f)$  of the neutral 44BPY $^0$  and anion species along the coordinate  $Q_f$  of the floppy degree of freedom computed for several basis sets. For the neutral species, the curves computed with the basis sets 6-31+g(d) and aug-cc-pVTZ are practically indistinguishable. Notice the fact that, unlike  $E_N(Q_f)$ , rather than the basis set size, the inclusion of diffuse basis functions is essential to correctly compute the adiabatic energy  $E_A(Q_f)$  of 44BPY $^{\bullet-}$ . Results obtained with the modest 6-31+g(d) basis set are reasonably good, while those with the basis set cc-pVTZ are not. See the main text for details.

## 5 44BPY in solvents

We have also extensively investigated the adiabatic energy surfaces of the neutral (44BPY $^0$ ) and charged (radical anion 44BPY $^{\bullet-}$  and radical cation 44BPY $^{\bullet+}$ ) species in the solvents utilized in experiments, e. g., aqueous solution,<sup>9,46</sup> toluene,<sup>47</sup> acetone,<sup>11</sup> 1,2,4-trichlorobenzene,<sup>48</sup> and acetonitrile.<sup>17</sup> In line with the preliminary investigation of Ref. 27, our calculations confirm the fact that, essentially, the solvent main effect is a nearly constant (i. e.,  $\mathbf{Q}$ -independent) shift with respect to the adiabatic surfaces of the corresponding species in vacuo. Therefore, we do not present adiabatic sur-

faces in various solvents. Rather, we restrict ourselves to report results for the aforementioned energy shift, which is important for molecular transport; the relative molecular orbital alignment with respect to the electrode Fermi levels is a key parameter that affects the current.<sup>49</sup>

In Table 1, we present the computed influence of the solvents listed above on the vertical ionization potentials ( $IP = E_C - E_N = -E_{HOMO}$ , where the subscript  $C$  stands for radical cation) and the vertical electron affinities ( $EA = E_N - E_A = -E_{LUMO}$ ) at the neutral equilibrium geometry. Although the 44BPY-based molecular junctions fabricated so far do not seem to exhibit hole-type (HOMO-mediated) conduction, we have also included results for the radical cation 44BPY<sup>•+</sup> and for the HOMO in order to point out an aspect, which is quite significant for the molecular transport in solvents.

As visible in Table 1, the IP and EA-shifts are substantial and significantly dependent on the solvent. As a consequence, the HOMO-LUMO gap  $W_{hl}$  is significantly affected by the solvents. Instead of estimating this gap from the HOMO and LUMO Kohn-Sham (KS) “orbitals” (whose physical meaning is questionable<sup>50</sup>), in Table 1 we have determined it from  $\Delta$ -DFT calculations as  $W_{hl} = IP - EA = E_C + E_A - 2E_N$ , an expression which shows that it is the counterpart of what is called the charge gap in solid state and mesoscopic physics (see, e. g., Refs. 27,51 and citations therein).

The point to which we want to draw attention here is that, although the solvent substantially affects the HOMO-LUMO gap, it causes HOMO and LUMO shifts in opposite directions, and their magnitudes are practically *equal*. The fact demonstrated here, that, for a given molecule (44BPY), a variety of solvents cause opposite HOMO- and LUMO-displacements of almost same magnitudes is complementary to another fact known earlier; the HOMO and LUMO displacements were found to be similar for a variety of (smaller) molecules in a given (namely, aqueous) solution.<sup>52</sup>

## 6 Impact of the twisted molecular conformation on the conductance

As already noted in Ref. 27 and reiterated above, unlike in the case of (practically) rigid molecules, the calculation of the electric current through molecular junctions based on floppy molecules requires a nontrivial step, namely an ensemble averaging in a nonequilibrium state.<sup>27</sup> This ensemble averaging is a problem on its own that will not be addressed in this paper.

Instead, we will briefly consider a simpler problem related to it: the dependence of the ohmic conductance  $G$  on the twisting angle  $\theta$ . Rather than examining changes in  $\theta$  due to molecular vibrations, in this section  $\theta$  will be considered as an independent geometrical parameter. This problem is also of interest; like in the case of the related biphenyl molecule,<sup>53,54</sup>

one can synthesize and investigate, e. g., derivatives of a molecular 44BPY series wherein the torsion angle  $\theta$  can be *tuned* by bridging the two pyridyl rings with alkyl chains of *variable* lengths.

The dependence  $G = G(\theta)$ , which has been considered theoretically for molecules consisting of two rings that can rotate relative to each other,<sup>35,55–60</sup> is interesting from the perspective of molecular conductance switching. Theoretically, an approximate dependence  $G \propto \cos^2 \theta$  has been found, which roughly agrees with experimental data in biphenyl-derivatives.<sup>53,54</sup> This behavior characterizes a molecular switch that is “on” and “off” in parallel ( $\theta = 0$ ) and perpendicular ( $\theta = 90^\circ$ ) conformations, respectively.

In spite of significant differences between existing approaches of the (ohmic) transport in 44BPY,<sup>11,33–35</sup> which are based on nonequilibrium Green’s function (NEGF) methods and the Landauer trace formula (see, e. g., Refs. 61–63), there is an important common finding in those studies. Namely, the fact that the coherent electron transport is determined by the LUMO: close to the metallic Fermi energy  $E_F$ , the calculated transmission exhibits a pronounced Lorentzian peak, which is well separated energetically from other peaks situated away from  $E_F$ . This single-level (“only LUMO”) model is simple but turned out to be realistic for 44BPY. By interpreting experimental thermopower data within this model, the LUMO was found to lie by  $\sim 1.53$  eV above the metallic Fermi energy, in good agreement with the theoretically estimated value of  $\sim 1.47$  eV.<sup>11</sup> So, we have a strong reason to accept this model, and then the low-bias conductance  $G$  can be expressed as (see, e. g., Refs. 61,64)

$$g(\theta) \equiv \frac{G(\theta)}{G_0} = \frac{\Gamma^2}{\tilde{E}_{LUMO}^2(\theta) + \Gamma^2} \simeq \frac{\Gamma^2}{\tilde{E}_{LUMO}^2(\theta)}. \quad (2)$$

Here  $\Gamma$  is a finite width due to the LUMO-electrode couplings,<sup>65</sup> which is usually much smaller than the LUMO-energy offset  $\tilde{E}_{LUMO}$  relative to the Fermi energy  $E_F$  of the electrodes to which the molecule is linked. The quantity  $\tilde{E}_{LUMO}$  differs from the difference between the value  $E_{LUMO}$  of the isolated molecule and  $E_F$ , because of the energy shift  $\delta E$  caused by molecule-electrode interactions (e. g., image charge effects<sup>66</sup>). We do not attempt to microscopically estimate here the difference between  $\tilde{E}_{LUMO}$  and  $E_{LUMO}$  ( $\tilde{E}_{LUMO} = E_{LUMO} - E_F - \delta E$ ). We determine this shift by requiring that the value of  $\tilde{E}_{LUMO}(\theta_{eq})$  at the equilibrium value  $\theta = \theta_{eq}$  (cf. Table S1) coincides with that deduced experimentally  $\tilde{E}_{LUMO}(\theta_{eq}) \simeq 1.5$  eV for 44BPY junctions.<sup>11</sup> Based on the previous calculations,<sup>27</sup> which indicated that the metal (Au) atoms contacted to 44BPY essentially causes a constant ( $Q_f$ -independent) shift of the LUMO energy (compare Figs. 3a and 3c of Ref. 27), we will ignore the  $\theta$ -dependence of  $\tilde{E}_{LUMO}(\theta) - E_{LUMO}(\theta)$ . For the basis set aug-ccpVTZ, we thus deduced  $\tilde{E}_{LUMO}(\theta) - E_{LUMO}(\theta) \simeq 1.92$  eV.

Medium	$W_{hl}$	IP= $-E_{HOMO}$	EA= $-E_{LUMO}$	$\delta$ IP	$\delta$ EA	$\delta$ IP+ $\delta$ EA
vacuum	8.76; 8.69; 8.71	9.15; 9.13; 9.13	0.38; 0.44; 0.42	—	—	—
water	5.26; 5.21; 5.24	7.42; 7.41; 7.42	2.15; 2.21; 2.19	-1.73; -1.72; -1.71	1.77; 1.76; 1.77	0.04; 0.04; 0.06
toluene	6.73; 6.67; 6.68	8.13; 8.12; 8.12	1.40; 1.46; 1.44	-1.01; -1.01; -1.01	1.02; 1.01; 1.01	0.001; 0.0005; 0.003
acetone	5.40; 5.34; 5.37	7.48; 7.48; 7.49	2.08; 2.14; 2.12	-1.66; -1.66; -1.64	1.70; 1.70; 1.70	0.04; 0.04; 0.05
acetonitrile	5.32; 5.26; 5.29	7.44; 7.44; 7.45	2.12; 2.18; 2.16	-1.70; -1.69; -1.68	1.74; 1.74; 1.74	0.04; 0.04; 0.06
TCB	6.82; 6.75; 6.77	8.18; 8.17; 8.16	1.35; 1.41; 1.39	-0.97; -0.97; -0.97	0.97; 0.97; 0.97	0.0001; -0.0006; 0.002

**Table 1** Values for the HOMO-LUMO gaps  $W_{hl} \equiv E_{LUMO} - E_{HOMO}$ , ionization potentials IP, and electron affinities of the 44BPY molecule in vacuo and several solvents (TCB  $\equiv$  1,2,4-trichlorobenzene) computed with the basis sets 6-31+g(d); aug-cc-pVDZ; aug-cc-pVTZ, respectively. Differences between the values of a certain quantity in solvent and in vacuo are denoted by  $\delta$ . Notice the opposite signs and the almost equal magnitudes  $\delta$  IP  $\simeq -\delta$  EA of the changes in the ionization potentials and electron affinities caused by the solvents with respect to the values in vacuo. See the main text for details.

Further, in view of the fact that changes of the molecule-electrode contacts turn out to only weakly affect the torsional angle,<sup>67</sup> we will also neglect a possible  $\theta$ -dependence of  $\Gamma$ ; we do not expect a substantial change in the short-range (*contact*) interaction between the LUMO and electrodes by varying the *inter-ring* angle  $\theta$ . By employing the experimental values  $G(\theta_{eq})/G_0 = 0.00068$  and  $\tilde{E}_{LUMO}(\theta_{eq}) \simeq 1.5$  eV,<sup>11</sup> Eq. (2) yields the value  $\Gamma \simeq 0.039$  eV.

To obtain the LUMO energy  $E_{LUMO}(\theta)$  of the isolated molecule, we performed  $\Delta$ -DFT-calculations<sup>50</sup> and computed<sup>68</sup>

$$E_{LUMO}(\theta) = E_A(\theta; \mathbf{R}') - E_N(\theta; \mathbf{R}'). \quad (3)$$

For simplicity, we present results of the calculations carried out for various conformations by varying the torsion angle ( $\theta$ ) while freezing all the other geometrical parameters at the neutral equilibrium geometry (denoted by  $\mathbf{R}'$ ).<sup>69</sup> Results illustrating the  $\theta$ -dependence of the LUMO energy  $E_{LUMO}(\theta)$  of the isolated molecule are shown in Fig. 7.

Once  $\tilde{E}_{LUMO}(\theta)$  is known, the  $\theta$ -dependence of the conductance can be deduced by means of Eq. (2). The dependence of  $G$  on  $\cos^2 \theta$  is shown in Fig. 8. As visible there, our result does not give support to the proportionality  $G \propto \cos^2 \theta$  found experimentally for other molecules<sup>53,54</sup> and DFT-based theories approaches.<sup>35,58,60</sup> Our results agree very well with the following Ansatz, which straightforward generalizes the aforementioned relationship

$$G(\theta)/G_0 = g_{\perp} + (g_{\parallel} - g_{\perp}) \cos^2 \theta. \quad (4)$$

It is worth emphasizing at this point the fact that in 44BPY the relationship  $G \propto \cos^2 \theta$ , which yields a perfect “off” switch  $G(\theta = 90^\circ) \equiv 0$ , is contradicted by a detailed microscopical analysis.<sup>55</sup> According to Ref. 55, the transmission through 44BPY remains nonvanishing even in a strictly perpendicular conformation, due to the existence of crossed  $\sigma - \pi$  electronic interaction.<sup>55</sup> According to the present estimation,  $g_{\perp} \simeq g_{\parallel}/3$ .

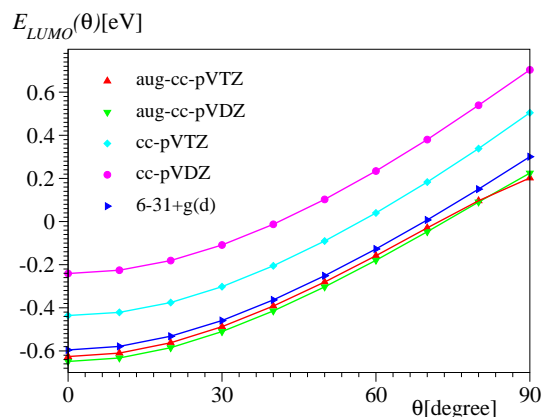


**Fig. 7**  $\Delta$ -DFT results for the LUMO energy of the 44BPY molecule computed with several basis sets (specified in the inset). Notice the importance of the diffuse functions. See the main text for details.

We end this sections with two remarks. First, we emphasize the difference between our present  $\Delta$ -DFT-based calculations and most DFT-approaches, wherein mathematical objects, namely KS orbitals, are treated as if they were real physical orbitals. Second, we note the relationship of the  $\theta$ -dependence discussed above and the very small energy barrier associated to the profile of the torsional potential, which is  $E_N(\theta)$  in our notation. An important issue amply discussed in the past (see, e. g., Refs. 18,19 and citations therein) is the magnitude of the barrier heights between the twisted global minimum and the planar and perpendicular conformers,  $\Delta E_0 \equiv E_N(\theta = 0^\circ) - E_N(\theta_{eq})$  and  $\Delta E_{90} \equiv E_N(\theta = 90^\circ) -$

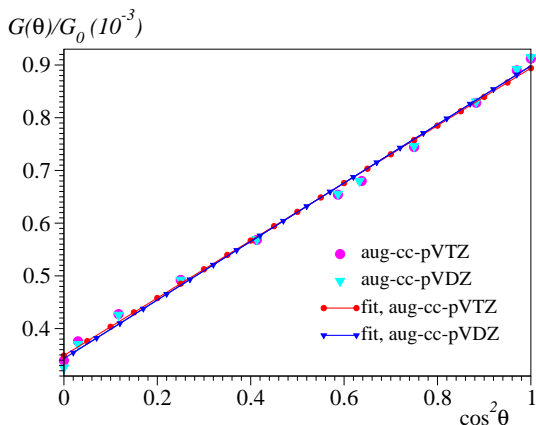


**Fig. 8** Dependence of the conductance  $G$  in units of conductance quantum  $G_0 = 2e^2/h = 77.5 \mu\text{S}$  on the torsional angle  $\theta$  obtained by using the basis sets specified in the inset. For each basis set, the conductance has been fixed at the experimental value  $G(\theta_{eq})/G_0 = 0.00068$ <sup>11</sup> ( $\theta_{eq} = 37.01$  for aug-cc-pVDZ and  $\theta_{eq} = 37.3$  for aug-cc-pVTZ, cf. Table S1). The straight lines have been obtained by fitting the results of quantum chemical calculations using the Ansatz of Eq. (4). The fact that the symbols corresponding to the various basis sets employed are hardly distinguishable from each other demonstrates the reliability of the results. See the main text for details.

$E_N(\theta_{eq})$ , respectively. The most recent calculations published so far<sup>19</sup> succeeded to produce values  $\Delta E_0 \simeq 1.5 \text{ kcal/mol}$  and  $\Delta E_{90} \simeq 2.2 \text{ kcal/mol}$ , which agree with the ordering  $\Delta E_0 < \Delta_{90}$  deduced from measured NMR spectra of 44BPY dissolved in nematic liquid crystal.<sup>70</sup> However, there still remain significant differences between theory and experiment; proton NMR measurements estimated  $\Delta E_0 \simeq 4.0 \text{ kcal/mol}$ .<sup>71</sup> Internal rotational barriers of heights comparable to 44BPY have also been found for other molecular systems.<sup>72,73</sup>

## 7 Discussion and Conclusions

In this paper, we have reported results of extensive quantum chemical calculations for the 44BPY molecule in vacuo and in different solvents employed in relevant experiments.

The small differences between the measured properties of the neutral 44BPY<sup>0</sup> and radical anion 44BPY<sup>•-</sup> and those, nearly convergent with respect to the basis set size, calculated within the DFT/B3LYP presented in the Electronic Supple-

mentary Information are representative for the present state-of-the-art of the theory: on one side, it demonstrate its rather high accuracy and, on the other side, that intrinsic limitations remain.

The results on the adiabatic energy curves and on the solvent effects presented in this work can (and will) serve as input information for subsequent transport studies through 44BPY-based molecular junctions.

Because, as expressed by the title, the remote goal of the present investigation is the molecular transport, three findings of this work are particularly worth to emphasize.

(i) We are not aware of attempts to microscopically incorporate solvent effects into transport approaches. Available program packages do not allow to perform microscopic transport calculations through molecular devices immersed in electrolytes. Our results indicate that the solvent acts as a *selective* gate electrode: it causes energy shifts of particle-like and hole-like orbitals in *opposite* directions and nearly same magnitudes. On this basis, we propose to embody solvent effects on molecular transport within a procedure based on a scissor operator. Let us remind at this point that the scissor operator technique has been proposed<sup>74</sup> and applied<sup>75–80</sup> in semiconductors to empirically cut the band structure along the band gap and rigidly move the energies of the conduction and valence bands in opposite directions. There, the scissor operator has been motivated technically, as an (empirical) correction of the band gap, whose value is underestimated by the DFT. More recently, a scissor operator has been utilized in molecular electronics<sup>11,81,82</sup> with both a technical and a physical motivation: to correct the too narrow KS HOMO-LUMO gap and to account for the energy shift due to electrodes via image effects,<sup>66</sup> respectively. For simplicity, in those approaches the HOMO and all occupied orbitals, and the LUMO and all unoccupied orbitals are shifted in opposite directions by the same quantity  $\Delta/2$  (half the correction to the HOMO-LUMO gap).

Similar to those discussed above, we also propose to account for solvent effects on the molecular transport by means of a scissor operator: the energies of the occupied and unoccupied orbitals should be moved by  $-\delta \text{IP}$  and by  $-\delta \text{EA}$ , respectively. Unlike in the aforementioned cases, wherein the assumption that the opposite shifts have the *same* magnitude ( $\Delta/2$ ) is merely done for convenience, our results give a microscopic support to the fact that the shifts are opposite and have practically the *same* magnitude  $-\delta \text{IP} \simeq +\delta \text{EA}$ . Notice that (a)  $\delta \text{IP}$  and  $\delta \text{EA}$  are not empirical quantities but deduced from quantum chemical calculations, and (b) the presently proposed scissor operator procedure can be applied on top of any transport approach in vacuo, let it be a ‘DFT+ $\Sigma$ ’ implementation<sup>11,81,82</sup> or else.

(ii) The results presented here (Figs. 6 and 7) clearly demonstrate that, in order to correctly describe the anion (thence the LUMO), it is necessary to employ basis sets that

include diffuse basis functions. Even by using basis sets of double zeta quality (cc-pVDZ), the omission of the diffuse functions, as often the case in many transport calculations, may yield errors  $\sim 0.4 - 0.5$  eV in the LUMO energy offset. In view of the fact that typical energy offsets amount  $\sim 0.6 - 1.5$  eV,<sup>11,64,83,84</sup> such errors in determining the LUMO location are unacceptably large.

(iii) Along with molecular junctions wherein a single 44BPY molecule is directly linked to electrodes,<sup>9,11,46,47</sup> molecular junctions wherein spacers (e. g., six alkyl units at either side<sup>10</sup>) are used to link the 44BPY molecule to electrodes are also of experimental interest. Because the largest basis sets employed in the present work may become a challenge for such molecular sizes, it is important to note that, once diffuse basis functions are included, anionic species can still be reliably described with rather modest basis sets, as illustrated by the results obtained by employing the 6-31+g(d) basis set shown in Figs. 6 and 7 and Table 1.

Figs. 6 and 7 present results demonstrating both the importance of (a) the diffuse basis functions and of (b) the most salient structural feature of the 44BPY molecule, namely the twisting inter-ring angle. One should emphasize that these two aspects are distinct from each other. Concerning aspect (a), one should note that diffuse functions are needed for the correct description of the anion. The errors introduced by using basis sets without diffuse functions, e. g., at the neutral equilibrium geometry ( $Q_f = 0$  in Fig. 6 or  $\theta = \theta_{eq} \simeq 37^\circ$  in Fig. 7) are practically the same as those far away from it (cf. Figs. 6 and 7). Concerning aspect (b), we remind what was already stated in Ref. 27 (see especially the next-to-last section of that work): the floppy degree of freedom ( $Q_f$ ) as well as its strong anharmonicity and significant reorganization energy are properties of the 44BPY molecule, which are affected neither by solvents nor by electrodes. Computations for 44BPY<sup>0</sup> and 44BPY<sup>•-</sup> immersed in solvents and by attaching gold atoms at the two ends show that the main effect is a practically constant shift of the anionic adiabatic energy surface with respect to the anion placed in vacuo.

To account for the effect of the intramolecular reorganization related to the floppy degree of freedom on the electron transport through 44BPY-based junctions, one should perform an ensemble averaging on a molecular system at away from equilibrium (nonvanishing external bias), which is a nontrivial problem.<sup>27</sup> As a preliminary step in demonstrating the significant impact of molecular conformation on the transport, we have presented results for the linear (ohmic) conductance as a function of the torsional angle  $G = G(\theta)$ . Our results obtained by quantum chemical calculations are well described by a phenomenological Ansatz, Eq. (4).

To end, let us finally mention that, at  $\theta = 90^\circ$ , the 44BPY molecule ( $D_{2d}$  symmetry) becomes unstable against a Jahn-Teller distortion.<sup>55,85</sup> Therefore, significant deviations from

the above Ansatz may occur close to the perpendicular conformation. Obviously, this is an issue that escapes the present considerations.

**Acknowledgments** Financial support from the Deutsche Forschungsgemeinschaft is gratefully acknowledged.

## Notes and references

- 1 C. L. Bird and A. T. Kuhn, *Chem. Soc. Rev.*, 1981, **10**, 49–82.
- 2 P. M. S. Monk, *The Viologens: Physicochemical Properties, Synthesis and Applications of the Salts 4,4'-Bipyridine*, Wiley, Chichester, 2001.
- 3 L. A. Summers, *The Bipyridinium Herbicides*, Academic Press, London, 1981.
- 4 M. Graetzel, *Acc. Chem. Res.*, 1981, **14**, 376–384.
- 5 P.-P. Knops-Gerrits, D. De Vos, F. Thibault-Starzyk and P. A. Jacobs, *Nature*, 1994, **369**, 543–546.
- 6 M. Vitale, N. B. Castagnola, N. J. Ortins, J. A. Brooke, A. Vaidyalngam and P. K. Dutta, *J. Phys. Chem. B*, 1999, **103**, 2408–2416.
- 7 S. Saha and J. F. Stoddart, *Chem. Soc. Rev.*, 2007, **36**, 77–92.
- 8 F. Cunha, N. J. Tao, X. W. Wang, Q. Jin, B. Duong and J. D'Agnesse, *Langmuir*, 1996, **12**, 6410–6418.
- 9 B. Xu and N. J. Tao, *Science*, 2003, **301**, 1221–1223.
- 10 I. V. Pobelov, Z. Li and T. Wandlowski, *J. Am. Chem. Soc.*, 2008, **130**, 16045–16054.
- 11 J. R. Widawsky, P. Darancet, J. B. Neaton and L. Venkataraman, *Nano Letters*, 2012, **12**, 354–358.
- 12 M. J. Frisch, G. W. Trucks, H. B. Schlegel, G. E. Scuseria, M. A. Robb, J. R. Cheeseman, G. Scalmani, V. Barone, B. Mennucci, G. A. Petersson, H. Nakatsuji, M. Caricato, X. Li, H. P. Hratchian, A. F. Izmaylov, J. Bloino, G. Zheng, J. L. Sonnenberg, M. Hada, M. Ehara, K. Toyota, R. Fukuda, J. Hasegawa, M. Ishida, T. Nakajima, Y. Honda, O. Kitao, H. Nakai, T. Vreven, J. A. Montgomery, Jr., J. E. Peralta, F. Ogliaro, M. Bearpark, J. J. Heyd, E. Brothers, K. N. Kudin, V. N. Staroverov, T. Keith, R. Kobayashi, J. Normand, K. Raghavachari, A. Rendell, J. C. Burant, S. S. Iyengar, J. Tomasi, M. Cossi, N. Rega, J. M. Millam, M. Klene, J. E. Knox, J. B. Cross, V. Bakken, C. Adamo, J. Jaramillo, R. Gomperts, R. E. Stratmann, O. Yazyev, A. J. Austin, R. Cammi, C. Pomelli, J. W. Ochterski, R. L. Martin, K. Morokuma, V. G. Zakrzewski, G. A. Voth, P. Salvador, J. J. Dannenberg, S. Dapprich, A. D. Daniels, O. Farkas, J. B. Foresman, J. V. Ortiz, J. Cioslowski, and D. J. Fox, Gaussian, Inc., Wallingford CT, 2010 Gaussian 09, Revision B.01.
- 13 V. Barone, F. Lelj, C. Cauletti, M. N. Piancastelli and N. Russo, *Mol. Phys.*, 1983, **49**, 599–619.
- 14 V. Barone, F. Lelj, L. Comisso, N. Russo, C. Cauletti and M. Piancastelli, *Chem. Phys.*, 1985, **96**, 435–445.
- 15 H. Kihara and Y. Gondo, *J. Raman Spectrosc.*, 1986, **17**, 263–267.
- 16 G. Buntinx, P. Valat, V. Wintgens and O. Poizat, *J. Phys. Chem.*, 1991, **95**, 9347–9352.
- 17 L. Ould-Moussa, O. Poizat, M. Castellà-Ventura, G. Buntinx and E. Kassab, *J. Phys. Chem.*, 1996, **100**, 2072–2082.
- 18 M. Castellà-Ventura and E. Kassab, *J. Raman Spectr.*, 1998, **29**, 511–536.
- 19 Ángel J. Pérez-Jiménez, J. C. Sancho-García and J. M. Pérez-Jordá, *J. Chem. Phys.*, 2005, **123**, 134309.
- 20 Z. Zhuang, J. Cheng, X. Wang, B. Zhao, X. Han and Y. Luo, *Spectrochim. Acta A*, 2007, **67**, 509–516.
- 21 D. Jose and A. Datta, *Crystal Growth & Design*, 2011, **11**, 3137–3140.
- 22 E. Kassab and M. Castellà-Ventura, *J. Phys. Chem. B*, 2005, **109**, 13716–13728.
- 23 The notation “(+\*)” means that diffuse and polarization functions have been added only to the nitrogen atoms.

- 24 A. Almenningen and O. Bastiansen, *Skr. K. Nor. Vidensk. Selsk.*, 1958, **4**, 1. We refer to the results of this work as cited, e. g., in Ref. 17.
- 25 F. Mata, M. J. Quintana and G. O. Sorensen, *J. Mol. Struct.*, 1977, **42**, 1–5.
- 26 M. Dewar and H. Schmeising, *Tetrahedron*, 1959, **5**, 166–178.
- 27 I. Báldea, *EPL (Europhy. Lett.)*, 2012, **99**, 47002.
- 28 C. Lapouge, G. Buntinx and O. Poizat, *J. Phys. Chem. A*, 2002, **106**, 4168–4175.
- 29 Thanks are due to Annika Bande for help to calculate the bond orders.
- 30 A. P. Scott and L. Radom, *J. Phys. Chem.*, 1996, **100**, 16502–16513.
- 31 P. Sinha, S. E. Boesch, C. Gu, R. A. Wheeler and A. K. Wilson, *J. Phys. Chem. A*, 2004, **108**, 9213–9217.
- 32 In comparison with the case of 44BPY<sup>•-</sup>, both the basis set size and the solvent have a much weaker effect on the Raman spectrum of 44BPY<sup>0</sup>.<sup>86</sup>
- 33 S. Hou, J. Zhang, R. Li, J. Ning, R. Han, Z. Shen, X. Zhao, Z. Xue and Q. Wu, *Nanotechnology*, 2005, **16**, 239.
- 34 R. Stadler, K. S. Thygesen and K. W. Jacobsen, *Phys. Rev. B*, 2005, **72**, 241401.
- 35 A. Bagrets, A. Arnold and F. Evers, *J. Am. Chem. Soc.*, 2008, **130**, 9013–9018.
- 36 In transport, the notion of “LUMO”/“HOMO” is slightly different from that of the conventional molecular orbital theory. “LUMO” and “HOMO” refer to the ground (electronic) states of a system (anion/cation) having an extra/missing electron ( $\mathcal{N} + 1/\mathcal{N} - 1$  electrons) with respect to the neutral system with  $\mathcal{N}$  electrons. The “LUMO”/“HOMO” energies needed in transport calculations, which enter the denominators of the Lehmann representation of the Green’s functions, are exactly expressed as differences of the corresponding ground state energies,  $E_{LUMO} = E_0(\mathcal{N} + 1) - E_0(\mathcal{N}) \equiv E_A - E_N$  and  $E_{HOMO} = E_0(\mathcal{N}) - E_0(\mathcal{N} - 1) \equiv E_N - E_C$ . See Eq. (7.55)–(7.57) in Ref. 87, pp. 74–75. These “LUMO” and “HOMO” used in transport would coincide with those employed in conventional quantum chemistry if the single-particle description were exact.
- 37 J. Zhang, Q. Chi, T. Albrecht, A. M. Kuznetsov, M. Grubb, A. G. Hansen, H. Wackerbarth, A. C. Welinder and J. Ulstrup, *Electrochimica Acta*, 2005, **50**, 3143–3159.
- 38 R. A. Marcus and N. Sutin, *Biochim. Biophys. Acta*, 1985, **811**, 265–322.
- 39 R. A. Marcus, *Rev. Mod. Phys.*, 1993, **65**, 599–610.
- 40 M. M. Toutounji and M. A. Ratner, *J. Phys. Chem. A*, 2000, **104**, 8566–8569.
- 41 W. Schmickler, *Surf. Sci.*, 1993, **295**, 43–56.
- 42 A. N. Kuznetsov and W. Schmickler, *Chem. Phys.*, 2002, **282**, 371–377.
- 43 I. G. Medvedev, *J. Electroanal. Chem.*, 2007, **600**, 151–170.
- 44 W. Schmickler, *Electrochimica Acta*, 1996, **41**, 2329–2338.
- 45 M. J. Bramley and T. Carrington Jr., *J. Chem. Phys.*, 1994, **101**, 8494–8507.
- 46 X. Li, B. Xu, X. Xiao, X. Yang, L. Zang and N. Tao, *Faraday Discuss.*, 2006, **131**, 111–120.
- 47 Xu, Xiao, X. Yang, L. Zang and Tao, *J. Am. Chem. Soc.*, 2005, **127**, 2386–2387.
- 48 J. R. Widawsky, M. Kamenetska, J. Klare, C. Nuckolls, M. L. Steigerwald, M. S. Hybertsen and L. Venkataraman, *Nanotechnology*, 2009, **20**, 434009.
- 49 F. Zahid, M. Paulsson and S. Datta, *Advanced Semiconductors and Organic Nano-Techniques*, Academic Press, 2003, vol. 3.
- 50 R. O. Jones and O. Gunnarsson, *Rev. Mod. Phys.*, 1989, **61**, 689–746.
- 51 I. Báldea and L. S. Cederbaum, *Phys. Rev. B*, 2008, **77**, 165339.
- 52 R. G. Pearson, *J. Am. Chem. Soc.*, 1986, **108**, 6109–6114.
- 53 L. Venkataraman, J. E. Klare, C. Nuckolls, M. S. Hybertsen and M. L. Steigerwald, *Nature*, 2006, **442**, 904–907.
- 54 D. Vonlanthen, A. Mishchenko, M. Elbing, M. Neuburger, T. Wandlowski and M. Mayor, *Angew. Chem. Int. Ed.*, 2009, **48**, 8886–8890.
- 55 S. Woitellier, J. Launay and C. Joachim, *Chem. Phys.*, 1989, **131**, 481–488.
- 56 V. Mujica, A. Nitzan, Y. Mao, W. Davis, M. Kemp, A. Roitberg and M. A. Ratner, *Adv. Chem. Phys.*, John Wiley & Sons, Inc., 1999, vol. 107, pp. 403–429.
- 57 W. Haiss, C. Wang, I. Grace, A. S. Batsanov, D. J. Schiffrin, S. J. Higgins, M. R. Bryce, C. J. Lambert and R. J. Nichols, *Nat. Mater.*, 2006, **5**, 995–1002.
- 58 C. A. Brito Silva, S. J. S. da Silva, E. R. Granhen, J. F. P. Leal, J. Del Nero and F. A. Pinheiro, *Phys. Rev. B*, 2010, **82**, 085402.
- 59 H. Song, M. A. Reed and T. Lee, *Adv. Mater.*, 2011, **23**, 1583–1608.
- 60 M. Bürkle, J. K. Viljas, D. Vonlanthen, A. Mishchenko, G. Schön, M. Mayor, T. Wandlowski and F. Pauly, *Phys. Rev. B*, 2012, **85**, 075417.
- 61 S. Datta, *Quantum Transport: Atom to Transistor*, Cambridge Univ. Press, Cambridge, 2005.
- 62 S. Lakshmi, S. Dutta and S. K. Pati, *J. Phys. Chem. C*, 2008, **112**, 14718–14730.
- 63 I. Báldea, H. Köppel, R. Maul and W. Wenzel, *J. Chem. Phys.*, 2010, **133**, 014108.
- 64 I. Báldea, *Phys. Rev. B*, 2012, **85**, 035442.
- 65 The parameter  $\Gamma$  is important, because it depends on the nature of the molecule-electrode contacts. See, e. g., P. J. Mohan, A. Datta, S. S. Malajosyula and S. K. Pati, *J. Phys. Chem. B*, 2006, **110**, 18661–18664.
- 66 M.-C. Desjonqueres and D. Spanjaard, *Concepts in Surface Physics*, Springer Verlag, Berlin, Heidelberg, New York, 1996.
- 67 C. B. George, M. A. Ratner and J. B. Lambert, *J. Phys. Chem. A*, 2009, **113**, 3876–3880.
- 68 Because Eq. (3) may resemble a Franck-Condon approximation (“vertical” transition)<sup>40</sup>, it is worth emphasizing that the physical mechanism underlying Eq. (2) is the coherent (adiabatic) electron transport, wherein the two electron transfer processes (say, source-molecule and molecule-drain) cannot be separated. This is distinct from the nonadiabatic transport described within the Mulliken-Hush-Marcus picture<sup>38–40</sup>, wherein the two aforementioned charge transfer processes proceed incoherently.
- 69 This is a possible manner of considering  $\theta$ -variations. The  $\theta$ -dependence of the results presented in this section do not significantly change by performing a full geometry optimization at fixed  $\theta$ . In that case, 44BPY<sup>0</sup> was found to be stable only for  $19^\circ \lesssim \theta \lesssim 64^\circ$ <sup>86</sup>. Anyway, both aforementioned manners of varying  $\theta$  are schematic. More elaborate microscopic calculations, by considering, e. g., bridging alkyl chains of variable lengths can be done, but this numerical effort is not justified at present because of missing experimental data for bipyridine-derivatives.
- 70 J. W. Emsley, D. S. Stephenson, J. C. Lindon, L. Lunazzi and S. Pulga, *J. Chem. Soc., Perkin Trans. 2*, 1975, 1541–1544.
- 71 Y. S. Mangutova, L. S. Mal’tseva, F. G. Kamaev, B. V. Leont’ev, S. Mikhamedkhanova, O. S. Otroshchenko and A. S. Sadykov, *Izv. Akad. Nauk. USSR, Ser. Khim.*, 1973, **7**, 1510. We refer to the results of this work as cited in Ref. 19.
- 72 S. Tsuzuki, T. Uchamaru, K. Matsumura, M. Mikami and K. Tanabe, *J. Chem. Phys.*, 1999, **110**, 2858–2861.
- 73 D. Jose and A. Datta, *J. Phys. Chem. Lett.*, 2010, **1**, 1363–1366.
- 74 G. A. Baraff and M. Schlüter, *Phys. Rev. B*, 1984, **30**, 3460–3469.
- 75 R. W. Godby, M. Schlüter and L. J. Sham, *Phys. Rev. B*, 1988, **37**, 10159–10175.
- 76 Z. H. Levine and D. C. Allan, *Phys. Rev. Lett.*, 1989, **63**, 1719–1722.
- 77 F. Gygi and A. Baldereschi, *Phys. Rev. Lett.*, 1989, **62**, 2160–2163.
- 78 V. Fiorentini and A. Baldereschi, *Phys. Rev. B*, 1995, **51**, 17196–17198.
- 79 X. Gonze, P. Ghosez and R. W. Godby, *Phys. Rev. Lett.*, 1995, **74**, 4035–4038.
- 80 X. Gonze and C. Lee, *Phys. Rev. B*, 1997, **55**, 10355–10368.
- 81 J. B. Neaton, M. S. Hybertsen and S. G. Louie, *Phys. Rev. Lett.*, 2006, **97**, 216405.
- 82 S. Y. Quek, L. Venkataraman, H. J. Choi, S. G. Louie, M. S. Hybertsen

---

and J. B. Neaton, *Nano Letters*, 2007, **7**, 3477–3482.  
83 I. Báldea, *Chem. Phys.*, 2012, **400**, 65–71.  
84 I. Báldea, *J. Am. Chem. Soc.*, 2012, **134**, 7958–7962.  
85 J. W. Lauher, *Inorg. Chim. Acta*, 1980, **39**, 119 – 123.

86 I. Báldea (unpublished).  
87 A. L. Fetter and J. D. Walecka, *Quantum Theory of Many Particle Systems*, McGraw Hill, New York, 1971.

---